

## Diamond-like carbon deposition by laser ablation

Camps E., Escobar-Alarcón L., Espinoza M. E.  
*Instituto Nacional de Investigaciones Nucleares*  
 Apdo. Postal 18-1027, México DF 11801, México

Camacho-López M. A.  
*Universidad Autónoma Metropolitana-I, Depto. De Física*

Rodil S. E. Muhl S.  
*Instituto de Investigaciones en Materiales, UNAM*

The plasma plume generated during laser ablation of a carbon target (graphite 99.99%), is characterized by means of Optical Emission Spectroscopy (OES) and the Langmuir probe technique. Both techniques allow the determination of the mean kinetic energy of ions present in the plasma. Besides that, information about the excited species and the plasma density is obtained. Ablation is carried out using a Nd:YAG laser operated at the fundamental frequency with laser fluences in the range of 2 to 6 J/cm<sup>2</sup>. The main excited specie in the plasma is the C<sup>+</sup> (299.26 and 426.7 nm). The kinetic energy of these ions can be varied from 100 eV up to 500 eV, as a function of the used fluence. The plasma density varies from 2 x 10<sup>12</sup> cm<sup>-3</sup> up to 9 x 10<sup>13</sup> cm<sup>-3</sup>, depending on the fluence and on the target-probe distance. Different samples of amorphous carbon thin films were deposited using different plasma parameters. The films show a sp<sup>3</sup>/sp<sup>2</sup> ratio which depend on the plasma conditions: a higher ratio is obtained for high densities and medium ion kinetic energies (about 200 eV). A 60% sp<sup>3</sup> content, in some samples, could be obtained in these experiments. The deposited films were analyzed using Raman spectroscopy and EELS.

**Keywords:** Laser ablation; Diamond like carbon films; Raman spectroscopy; EELS

### 1. Introduction

Diamond-like carbon (DLC) films have attracted substantial attention recently [1-3] due to the wide spectrum of potential applications mainly in mechanical applications which take advantage of the high mechanical hardness, low friction, optical transparency and chemical inertness of the material, due to the presence of the C-C sp<sup>3</sup> bonds. The commercial use of DLC is at present as protective coatings for magnetic disk drives and anti-reflective protective coatings for IR windows [4]. These types of films can be produced by techniques such as, chemical vapour deposition (CVD) and pulsed laser deposition (PLD). The PLD technique is known to produce high sp<sup>3</sup>/sp<sup>2</sup> bond ratios, with low or no hydrogen content, and that the film characteristics depend on the growth conditions [5].

Diamond-like carbon can only be produced under specific deposition conditions. The theory of the growth models are based on the ideas originally proposed by Lifshitz [6]. According to Lifshitz carbon ions with sufficient energy are supposed to accumulate by subsurface implantation with an accompanying thermal spike. Another microscopic model has been proposed by Robertson [7], in which again subplantation is considered the underlying mechanism. In this model it was suggested that densification caused by the implantation promoted atomic hybridisations to adjust the local density, favouring the formation of sp<sup>2</sup>C in low-density regions and sp<sup>3</sup>C formation in the high-density regions. It is considered that subplantation of atoms can either occur by direct implantation of the incoming ions or

by knock-on implantation of the surface atoms. The accumulation of atoms in "interstitial" positions causes an increase in the local density and thus the local bonding transformations to sp<sup>3</sup> hybridisation to compensate. In order for the ion to penetrate the film, or cause knock-on implantation, it must have an energy above a certain threshold level. It was also suggested, however, that ions of much higher energies would not promote sp<sup>3</sup> hybridisation because they would cause damage or excessive local heating which could activate a relaxation in the excess density. Thus there exists an optimum ion energy for maximum sp<sup>3</sup> content, just above the penetration threshold.

The above discussion points to the fact that in order to deposit DLC films a detailed knowledge of the characteristics of the particles used to form the films is necessary. When plasmas are used, this means that a prior diagnostic study of the plasma parameters should be performed and this is one of the main aims of the present paper. This work employed Optical Emission Spectroscopy (OES) to study the main excited species present in the plasma during laser ablation of a carbon target. A planar Langmuir probe was used to quantify the mean energy and density of ions, in the position where the substrate was located. The third part of this work is related to the characterization of amorphous carbon films deposited using the diagnosed plasma regimes.

### 2. Experimental Setup

The deposition of the films and the analysis of the plasma were carried out in a device designed and constructed in

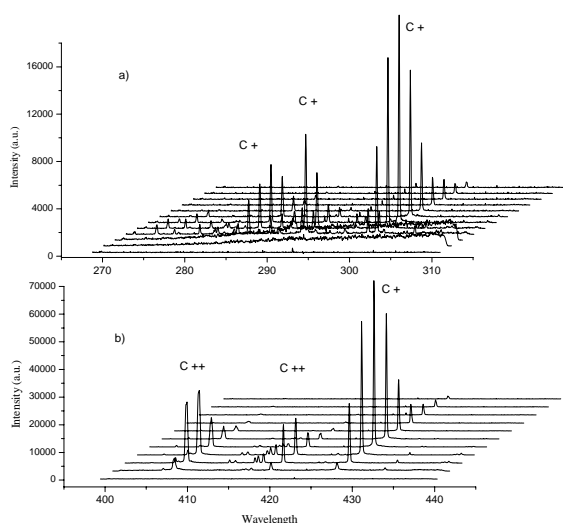


**Figure 1.** Time resolved optical emission spectra, for the two spectral regions where plasma emission was detected. The time step between spectra is 50 ns.

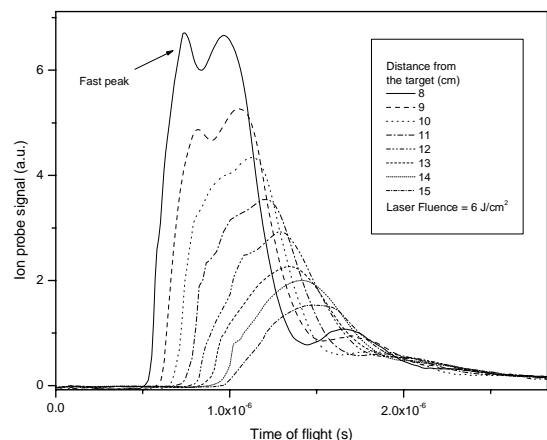


**Figure 2.** Time of flight curves of the ion current, detected with the Langmuir probe.

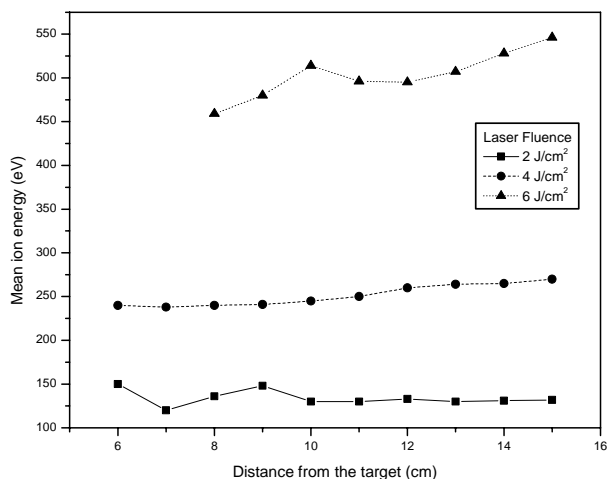


**Figure 3.** Mean ion kinetic energy as a function of the distance from the target for different values of laser fluence.

our laboratory, described in detail elsewhere [8]. Briefly, laser ablation was performed using a Q-switched Nd:YAG laser with emission at the fundamental line ( $\lambda = 1064 \text{ nm}$ ) with a 28 ns pulse duration. The energy delivered to the target could be varied from  $2 \text{ J/cm}^2$  to  $6 \text{ J/cm}^2$ . The laser beam was focused on the rotating high purity graphite

target at an incidence angle of  $45^\circ$ . The 150-mm-diameter vacuum chamber was evacuated to a base pressure of  $7 \times 10^{-6}$  Torr. In order to perform experiments at higher pressures, the vacuum chamber was filled with helium up to the necessary pressure.

Optical emission spectroscopy was carried out using a gated intensified CCD which allowed performing time resolved measurements for the different distances from the target, up to approximately 4 cm, where the plasma emission becomes undetectable. The light from the plasma was collected by a system of lenses, focused into a UV-Vis optical fibre bundle and transported to a 0.5 m spectrograph. A  $40 \mu\text{m}$  slit and a 1200 l/mm grating were used throughout. This arrangement allowed a 40 nm spectral window with a  $2 \text{ \AA}$  resolution.

A Langmuir planar probe that could be displaced along the propagation axis ( $x$  axis in the following,  $x=0$  is the target position) of the plasma plume was used to study the time of flight of plasma ions and for the determination of the plasma density. Data were recorded from 6 cm to 15 cm from the target surface. The probe consisted of a 3-mm diameter disk, and was biased with a fixed voltage at -30 V, where saturation of the ion current was evident. The signal from the probe was monitored through a load resistor of  $40 \Omega$  and recorded on a fast digital oscilloscope, HP54522A.

The amorphous carbon thin films were deposited on silicon and glass substrates cleaned in ultrasonic bath of methanol. In order to study the influence of plasma parameters on the characteristics of the deposited material, the films were deposited at different distances from the substrate between 6 and 15 cm, and three values of laser fluence, a low value of  $2 \text{ J/cm}^2$ , a medium value of  $4 \text{ J/cm}^2$  and a high one of  $6 \text{ J/cm}^2$ . The surface morphology of the samples was examined using a SEM equipped with a EDS probe which was used to ensure the absence of contamination. Raman spectroscopy measurements were performed at room temperature in air with a Spex 1403 double monochromator using the 514.5 line of an argon laser at a power level of 100 mW in the backscattering configuration. EELS was carried out using a Gatan Image Filtering attached to a JEOL 2010 TEM. The EELS spectra were acquired with a 200 kV energy, 0.3 dispersion, in the spectroscopic mode with a 2 mm aperture.

### 3. Results and discussion

#### a) Plasma diagnostics

Figures 1a and 1b show typical spectra with the spectrograph centered at 290 and 420 nm, respectively.

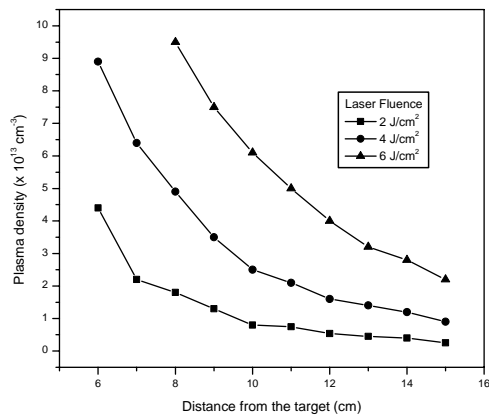


Figure 4. Plasma density as a function of the distance from the target for different values of laser fluence.

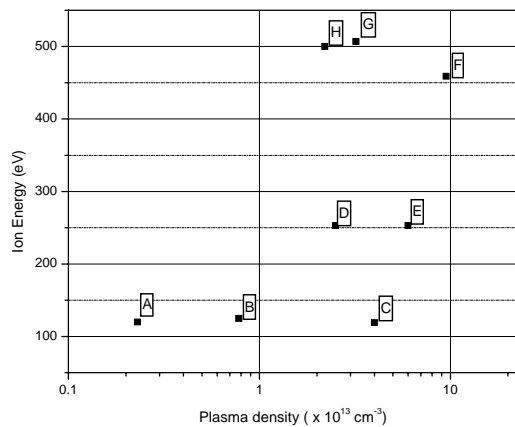


Figure 5. Mean ion energy – Plasma density diagram showing the experimental conditions under which samples were prepared.

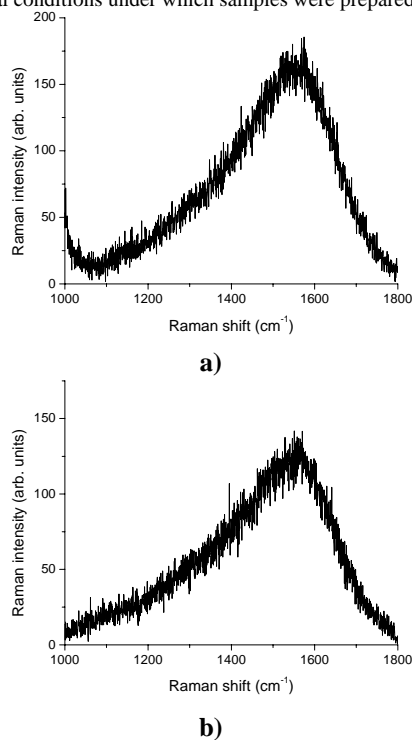
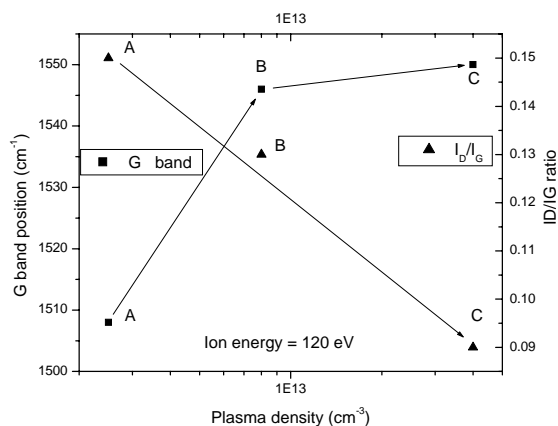


Figure 6. Raman spectra of amorphous carbon films. a) Sample D, b) sample B (see fig.5).

These figures show the temporal evolution of the emission at  $x = 0.5$  cm with a delay time step of 50 ns (i.e. time between strips) and at a pressure of  $7.5 \times 10^{-6}$  Torr. The emitting species are always the same, no matter what pressure or laser flux is used and they are;  $C^+$  (283.66, 290.6, 299.2 and 426.65 nm) and  $C^{++}$  (406.89 and 418.66), with the  $C^+$  being the most intense and that lived for the

longest times. Plotting the emission intensity vs. delay time, one can obtain the time of flight (TOF) spectra for each of the emission peaks and the mean kinetic energy of the species was calculated from those curves [9]. For the highest laser fluence used, the mean kinetic energy calculations were performed and they showed an overall behaviour that can be resumed as follows: the mean kinetic ion energy achieves its maximum value of 400 eV at approximately  $x = 2$  cm, then it remains constant. This result agrees well with results obtained with the probe for longer distances. For the purposes of the present paper the plasma characteristics far from the target are of importance, since as splashing is significantly reduced at such distances films with a very smooth morphology can be obtained.

The Langmuir Probe was used to obtain the TOF spectra of ions and their density, at different distances from the target. Fig. 2 shows a typical set of curves obtained for a fixed value of laser fluence and different distances from 8 to 15 cm from the target. From these spectra the mean kinetic energy of ions was obtained, following the procedure described in ref [9]. The plasma density values were obtained from the peak values of current of the TOF curves. Fig. 3 shows the mean ion kinetic energy as a function of the distance from the target, for different values of laser fluence. The ion energy remains practically constant for each value of fluence. For the higher fluence ( $6 \text{ J/cm}^2$ ) a higher ion energy (between 450 and 500 eV) was obtained. The lowest values of ion energy, of about 120 eV, were obtained for the low fluence. It is worth noting that a small increase in energy with distance was observed. This behaviour has been observed by other groups; particularly when higher (than in our case) fluences are employed [see e.g. 9, 10] and can be explained in terms of the existence of an acceleration mechanism inside the plasma due to the violation of the plasma quasi-neutrality, with this leading to the formation of an electric field which accelerates ions. This can be observed in the TOF curves as a fast peak in front of the main ion peak (see fig. 2). Fig. 4 shows the plasma density as a function of the distance from the target, for different values of laser fluence. It is seen from this plot that a higher flux and a smaller distance from the target results in a higher plasma density. In the range of distances studied with the probe the plasma density also depends on the working pressure, it decreases as the pressure is increased. Similarly, the plasma plume reduces in its dimensions and is confined to a smaller space, and furthermore, the particles that can escape from the region of the plasma plume are reduced as the pressure is increased. On the other hand, the ion energy has only a small dependence on the pressure; at least in the range of



**Figure 7.** Position of the Raman G peak and value of the ratio  $I_D/I_G$  as a function of the plasma density. The ion energy is kept constant at a value of 120 eV. A, B and C, are the analysed samples.

pressures studied in this work (from  $7.6 \times 10^{-6}$  to  $1 \times 10^{-2}$  Torr), the variation for fixed laser fluence was not greater than 50 eV.

The above results show that for the conditions in which the ablation of the carbon target is carried out in this work, the range of mean ion energy covers the values in which we can expect the formation of amorphous carbon thin films with a high content of  $sp^3$  C hybridisation.

#### b) Thin film deposition

Fig. 5 shows Ion energy – Plasma density diagram obtained by combining figs. 3 and 4. This diagram was used to determine the plasma conditions under which deposition of films were to be carried out. For example, point F, in fig. 5, means that sample number F, was deposited with a mean ion kinetic energy close to 450 eV and a plasma density equal to  $9.5 \times 10^{13} \text{ cm}^{-3}$ , and so on. From this figure it can be seen that three levels of ion energy were used. A high level with ion energy around 450 eV, a medium level with energies around 250 eV and a low one in which the ion energy had a value close to 120 eV. For each level of ion energy different values of plasma density were used to prepare the samples.

We used Raman spectroscopy to study the variation in the characteristic peaks D and G of amorphous carbon as a function of the deposition conditions. Fig. 6 shows two typical Raman spectra, in this case for samples B and D (plasma parameters for these samples are shown in fig.5), in order to obtain information from the Raman spectra, a fitting process must be carried out. The Raman spectra were interpreted in terms of the model proposed by Ferrari and Robertson [11]. For this model a Breit-Wigner-Fano + Lorentzian fitting was used to obtain the relation  $I_D/I_G$  (as the ratio of the peak heights) and the G peak position. Fig. 7 shows the variation of these quantities for the case of samples deposited at low fluence (i.e. low ion energy, samples A, B and C in fig.5) with different values of plasma density. From this plot it can be seen that when the

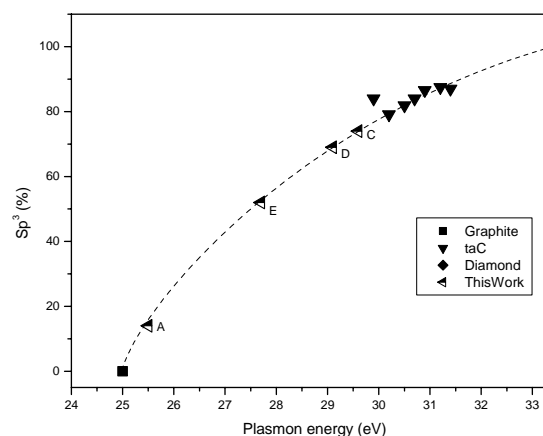


**Figure 8.**  $sp^3$  content as a function of the plasmon energy. For ta-C data were taken from [12]. The dashed line is a guide for the eye.

plasma density is increased (the ion energy is constant at 120 eV) the ratio  $I_D/I_G$  tends to decrease and the position of the G peak tends to increase. In other words, in this case as the plasma density increases the  $sp^3$  content in the film also tends to increase. For the case of the highest energies (samples F, G and H in fig. 5), the  $I_D/I_G$  ratio and the position of the G peak both tend to increase with the initial increase in the plasma density, but further increases in the density causes the  $I_D/I_G$  ratio to decrease and the position of the G peak to have only a small increase. This situation can be interpreted as follows: for the lowest plasma densities (with the energy at a high level) a polycrystalline graphite-like material without  $sp^3$  is formed, and with further increases in the plasma density the deposit becomes amorphous with preferential  $sp^2$  bonding with a very low  $sp^3$ . So, as might be expected, at high ion energies it was not possible to obtain a film with high  $sp^3$  content. When the plasma density is fixed at  $5 \times 10^{13} \text{ cm}^{-3}$  and the ion energy is increased from the low level values to the medium level values (samples C and D),  $I_D/I_G$  tends to decrease and the peak G moves to higher values. A further increase in ion energy reverses this tendency (samples D and G);  $I_D/I_G$  begins to increase and the G peak moves to smaller values. Therefore, in this case the  $sp^3$  content in the film slightly increases as the ion energy is increased up to the medium level value close to 250 eV, and at higher ion energies the excess energy promotes thermal relaxation reducing the effectiveness of the  $sp^2$  to  $sp^3$  transformation.

In order to verify the above-discussed Raman results, a few samples made under a selection of the conditions indicated in fig. 5, were analysed using Electron Energy Loss Spectroscopy. We used the value of the plasmon energy to characterize these films. From the low-energy-loss-spectrum part of the EELS, we measured the plasmon energy at the maximum intensity of the plasmon. It is well known that the plasmon energy is proportional to the  $sp^3$  content in the film. We used the results from other authors [12], who measured the  $sp^3$  content for some samples, including graphite and diamond, and constructed a plot

which shows the  $sp^3$  content as a function of the plasmon energy. Figure 8 shows this plot, where a dashed line was used to connect the points between graphite and diamond. On this line we can find the respective value of the  $sp^3$  content, for the plasmon values measured for the films deposited in this work.

According to the Raman analysis sample A should have  $sp^3$  content less than sample C, and sample D should have the same or slightly less  $sp^3$  content than sample C, this is in good agreement with EELS measurements shown in fig. 7.

#### 4. Conclusions

Analysis of the plasma plume produced by laser ablation of a carbon target revealed the presence of carbon ions with energies ranging from 100 eV up to 500 eV, with different plasma densities depending on the target-substrate distance. Under these conditions amorphous carbon thin films with different  $sp^3$  contents were deposited. The overall behaviour showed that the highest  $sp^3$  content is obtained when the lowest ion energy is used ( $\sim 120$  eV) together with the highest obtainable plasma density, i.e. when the lowest laser fluence is used. When the ion energy is increased the plasma density must be reduced to improve the  $sp^3$  content. A further increase in the ion energy produces films with low  $sp^3$  bonding even when the lowest plasma densities are used.

#### Acknowledgements

The present work was supported by the Consejo Nacional de Ciencia y Tecnología of Mexico under contracts 29250-E and 33873-E.

#### References

- [1]. D. R. McKenzie, *Rep. Prog. Phys.* **59**, 1611 (1996).
- [2]. R. Silva, G. A. J. Amaratunga, J. Robertson, W. I. Milne (Eds.) *Amorphous Carbon – State of the art*, World Scientific, Singapore, 1998.
- [3]. J. Robertson, *MRS Symposium proceedings*, 508 (1998).
- [4]. T. Yoshitake, H. Aoki, K. Suizu, K. Takahashi, K. Nagayama, *Appl. Surf. Sci.* **141**, 129 (1999).
- [5]. Voevodin, M. S. Donley, J. S. Zabinski, *Surf. & Coat. Technol.* **92**, 42 (1997).
- [6]. Y. Lifshitz, S. R. Kasi, J. W. Rabalais, *Phys. Rev. Lett.* **62**, 1290 (1989).
- [7]. J. Robertson, *Diamond Rel. Mater.*, **3**, 361 (1994).
- [8]. L. Escobar-Alarcón, M. Villagrán, E. Haro-Poniatowski, J. C. Alonso, M. Fernández-Guasti, E. Camps, *Appl. Phys. A*, **69**, s583 (1999).
- [9]. Nadezhda M. Bulgakova, Alexander V. Bulgakov, Oleg, F. Bobrenok, *Phys. Rev. E*, **62**, 5624 (2000).
- [10]. J. S. Pearlman, J. J. Thomson, and C. E. Max, *Phys. Rev. Lett.* **54**, 1397 (1977).
- [11]. C. Ferrari, J. Robertson, *Phys. Rev. B*, **61**, 14095 (2000).
- [12]. A. C. Ferrari, A. Libassi, B. K. Tanner, V. Stolojan, J. Yuan, S. E. Rodil, B. Kleinsorge and J. Robertson, *Phys. Rev. B*, **62**, 11089 (2000).